Knowledge E
Engaging minds

Conference Paper

Kinetics of Twinning and Dislocation Slip During Cyclic Deformation of ZK30 Magnesium Alloy

E. Vasilev[1], D. Merson[1], and A. Vinogradov[1,2]

[1]Institute of Advanced Technologies, Togliatti State University, Togliatti, 445667, Russia
[2]Department of Department of Mechanical and Industrial Engineering, Norwegian University of Science and Technology - NTNU, 7491 Trondheim, Norway

Abstract

The present study clarifies the anisotropy of tension-compression behaviour during the cyclic deformation of ZK30 magnesium alloy. Some details of mechanical twinning and dislocation slip are studied by acoustic emission technique and direct video observations. Through the combination of these methods, the overall effect of deformation mechanisms is determined for each loading direction and their effect on the cyclic deformation is highlighted.

Corresponding Author:
E. Vasilev
avellko@yandex.ru

Received: 10 February 2018
Accepted: 14 April 2018
Published: 7 May 2018

Publishing services provided by Knowledge E

Selection and Peer-review under the responsibility of the RFYS Conference Committee.

1. Introduction

Magnesium and its alloys are promising materials for many engineering applications due to their high specific strength and light weight [1]. There is still a lot of desire and plenty to improve in the mechanical properties of Mg alloys. Modern wrought Mg alloys suffer from poor ductility [2] and insufficient fatigue resistance [3]. The key reason for the detrimental mechanical properties of magnesium alloys is associated with the limited number of slip systems in the hexagonal close packed (hcp) crystal lattice. At low homologous temperatures, the dislocation slip is possible in the most closely packed direction $\langle 11\bar{2}0 \rangle$, or $\langle a \rangle$ slip, on basal (0001), prismatic $\{10\bar{1}0\}$ and pyramidal $\{10\bar{1}1\}$ planes [4, 5]. However, even when all basal and non-basal $\langle a \rangle$ systems are activated, they provide only four independent slip systems while the accommodation of arbitrary homogeneous deformation in polycrystalline aggregates requires activation of at least five independent deformation modes according to the von Mises-Taylor criterion [6]. Besides, none of these systems can accommodate plastic deformation perpendicular to the basal plane. Since the $\langle c + a \rangle$-slip in the second-order pyramidal system has a very high critical resolved shear stress (CRSS) at ambient temperatures, twinning is activated in Mg as an additional accommodation mechanism to satisfy the

von Mises-Taylor criterion [4, 5]. In magnesium, the most easily activated twinning modes are $\{10\bar{1}2\}$ extension and $\{10\bar{1}1\}$-type compression twinning [7]. The twinning on $\{10\bar{1}2\}$ plane is associated with extension along the *c*-axis and reorientation of the lattice by 86.3°. The $\{10\bar{1}1\}$ compression twinning results in contraction along the *c*-axis and tilting of the lattice by 56°. Due to the polar nature of twinning, a specific twinning system is favoured by only one direction of loading, i.e. tension or compression [7-9]. Therefore, magnesium responds quite anisotropically to mechanical loading, and plastic deformation of polycrystalline magnesium leads to the development of pronounced texture [2, 10, 11]. Upon reversal of the load direction, the twins shrink due to the motion of dislocations at the twin boundaries in opposite direction (de-twinning) and can disappear completely. Deformation twinning involves two steps: nucleation and growth of twin lamellae. De-twinning is associated with twin shrinkage [12]. This complexity of the mechanical response of Mg alloys is further exacerbated by the strong textures that are developed in magnesium alloys during thermo-mechanical processing. Therefore, the interplay between dislocation slip and twinning underlying the said complexity is not fully understood [4] and their role in cyclic deformation has yet to be rationalized.

Acoustic emission (AE) is gaining popularity among the materials scientists nowadays as tool of choice for real-time characterization of deformation mechanisms in solids. Due to its extraordinary high sensitivity to twin initiation [13] and unprecedented temporal resolution it has been proven effective for in-situ characterization of deformation behaviour of magnesium alloys [14-16]. The modern AE signal processing can provide detailed information about underlying deformation mechanisms such as dislocation slip and twinning even if these two operate simultaneously on different stages of loading [17, 18]. However, precise understanding of AE data is always a challenging task and the present work is aimed at gaining deeper insight in this area with the combined use of the advanced acoustic emission technique and direct microscopic video imaging.

2. Experimental section

The Mg-Zn-Zr alloy system is among the most know and most detailed studied since it exhibits a very attractive combination of functional properties including a reasonably high strength and ductility. Commercial purity ZK30 alloy with nominal compositions 2.6Zn-0.01Zr-Mg was twin-roll cast and subjected to a T4 thermomechanical treatment

involving annealing at 413 °C for 24 h in argon followed by air cooling. For metallographic observations, the specimens were mechanically polished down to 0.25 um and then etched in a solution containing 10 mL nitric acid and 90 mL ethanol. Microstructural observation was carried out using an optical microscope Zeiss Axiovert. The typical grain structures is after the thermal treatment shown in Figure 1 and one can notice a coarse grain (of 200 μm on average) uniform microstructure with randomly and uniformly distributed precipitates of secondary phases. The details of the microstructure and texture investigations will be reported elsewhere.

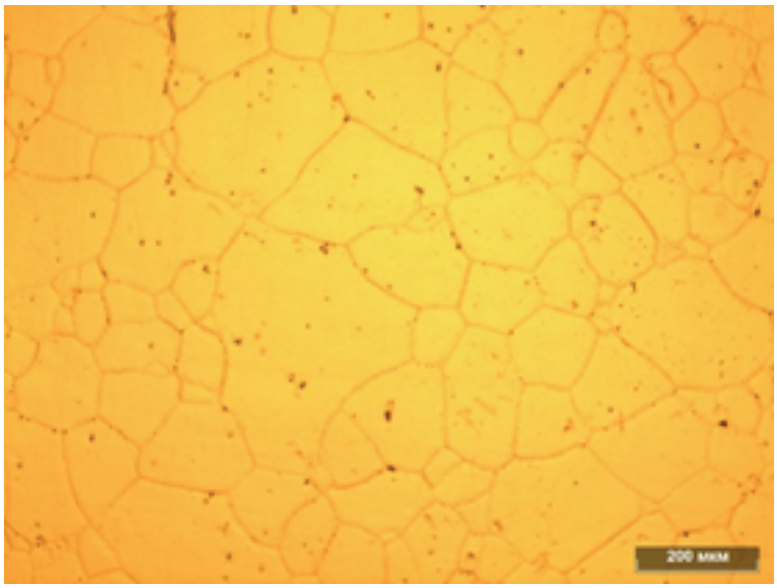

Figure 1: Optical micrograph showing microstructure of the rolled and annealed ZK30 alloy.

The experimental setup has been described in detail in [19]. Mechanical testing was carried out using the electro-mechanical testing machine Kammrath&Weiss with maximum load up to 10 kN. Cyclic tests were conducted on flat dog bone-shaped specimens having the gauge dimensions of 10x4x4 mm. The specimens were cut by spark erosion in the longitudinal direction of the TRC strips. They were mechanically polished to a mirror finish before testing. Axial push-pull deformation cycles were performed under total strain range $\Delta\epsilon_t = 0.02$ at the cross head velocity of 5 um×s^{-1} corresponding to the nominal strain rate $\dot{\epsilon} = 5\times10^{-4}$ s^{-1}. Video data has been recorded using a Pike 1 Mpixel camera at 30 frames-per-second rate.

A broadband AE sensor PICO was securely fixed on an unstrained shoulder part in close proximity to the gauge part. Silicon grease was used a coupling media between the specimen and the sensor to ensure the good acoustic contact. The AE signal was amplified by 60 dB in 30-1000 kHz range and then transferred to the PC-based AE acquisition system with PCI-2 board at the core (Physical Acoustics Corporation, USA).

The AE recording was performed in a threshold-less mode at a sampling rate of 2 MHz and resolution of 18 bit. To perform the AE signal categorization and identification of dominating deformation mechanisms, the continuously streamed data were sectioned into consecutive individual realizations of 1024 readings. A Fourier power spectral density (PSD) function $G(f)$ was calculated from these data using a Welch technique. The AE power (often termed "energy") was calculated from the corresponding PSDby definition $E = \int_{f_{\min}}^{f_{\max}} G(f)\,df$ and the median frequency f_m of the PSD function was introduced in terms of the implicit equation $\int_0^{f_m} G(f)\,df = \int_{f_m}^{\infty} G(f)\,df$ [17, 20]. The sectioned AE data set was analyzed employing the signal categorization technique - adaptive sequential *k*-means clustering (ASK) - proposed in [21]. The normalized power spectral density (PSD) function $\tilde{G}(f) = G(f)/E$ was used as input for the ASK algorithm, which compares the difference between them using a symmetrical version of the Kulback-Leibler divergence as a statistical measure of similarity between two data sets. The ASK procedure tries to join the signals with similar spectra into the compact groups and disjoin the signals having statistically different power spectral densities. It is important to notice that the ASK procedure is robust, non-supervised and data-driven. It means that as opposes to conventional clustering schemes such as *k*-means or *c*-means, we do not specify a priory how many clusters to be derived from the data set. Further details of the AE data processing can be found in [21] and [17]. As part of the implementation of the ASK algorithm, a set of descriptive variables is extracted for each AE realization. This set, in addition to the above mentioned energy and median frequency, includes the peak AE amplitude, the root mean square voltage, kurtosis of the waveform [22] and the power spectral density, etc. Besides, the number of elements belonging to specific clusters and their cumulative energy was computed and these quantities are used for visualization and comparative analysis of operative deformation mechanisms emitting AE.

The ASK algorithm has been proven extremely efficient in noise recognition and filtering. Using various Mg alloys it has been demonstrated in our earlier works that the noise signals are typically low-amplitude and low-energy with the PSD maximum in the low frequency domain below 100 kHz. The AE signals corresponding to twinning appear usually as high-power, high-amplitude transients which is opposite to low-amplitude noise-like smooth signals due to dislocation slip. The PSD for these two deformation modes is also different as will be discussed below.

3. Results and discussion

Significant asymmetry in the stress-strain curves during tension and compression of Mg alloys can be observed at the very first loading cycle, Figure 2. This asymmetry includes the difference in the yield stress, peak stress and hardening rate in tension and in compression, inelastic relaxation on unloading/reloading cycles, etc. Such an asymmetric behavior can be substantiated by concurrent activity of different mechanisms outlined above - slip, different variants of twining depending on the crystallographic orientation of individual grain and detwinning - however, understanding of temporal details of operation of these mechanisms is still far from being comprehensive.

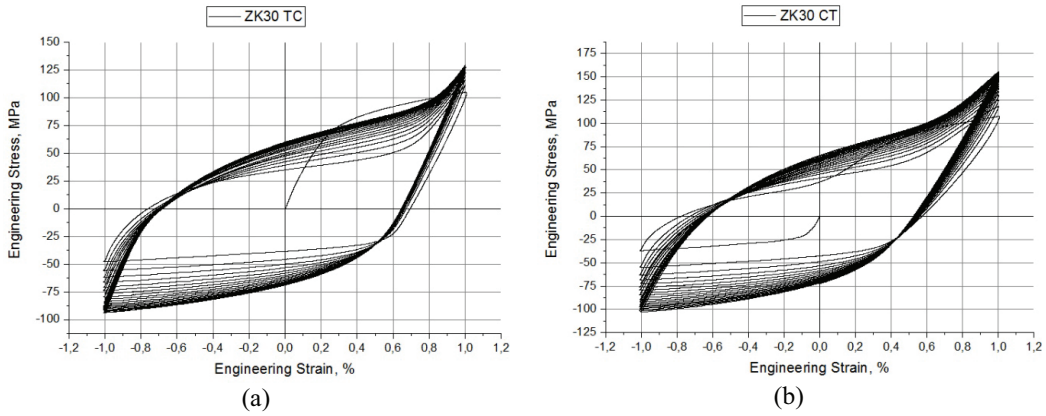

Figure 2: Cyclic hysteresis loop obtained during deformation of ZK30 alloy initially loaded: (a) in tension direction; (b) in compression direction.

3.1. Tension-compression cycle.

The analysis of images arranged in a chronological order through the first tension-compression cycle (Figure 2) shows that during tension the profuse dislocation slip occurs resulting in formation of a pronounced relief highlighting the grain boundaries (b-c); only scarce twin lamella are observed in favorably oriented grains on this stage. In contrast, intensive twinning takes place during the compression phase of the cycle (e-f); no visual traces of dislocation slip are observed. With unloading to zero level (j), some detwinning is observed after tension while there are no visual changes after compression (d).

The application of the ASK procedure to the AE time series recorded concurrently with the hysteresis loops shown in Figure 1a and video images shown in Figure 2 yields that all AE signals fall naturally into 3 major clusters, figures 3 and 4. According to these results, the AE cluster 1 can be undoubtedly attributed to background noise. The AE

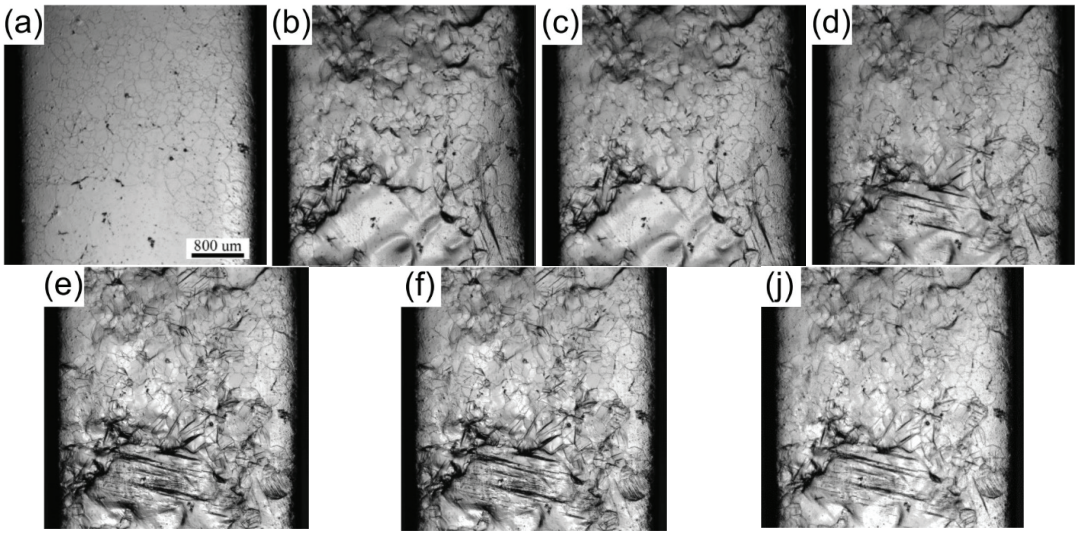

Figure 3: Successive optical video images for the first tension-compression cycle: (a) initial surface; (b) tension to 1% total strain; (c) unloading to 0 MPa; (d) unloading to 0% strain; (e) compression to -1% strain; (f) unloading to 0 MPa; (j) unloading to 0% strain.

recording started a few seconds (of 17 s) before the beginning of mechanical loading, which is clearly seen in Figure 4. Thus, the first AE records characterize the properties of laboratory noise and the AE signals differ from noise in accord to the conventional 3-sigma statistical criterion. As expected, noise signals are of low energy. Their PSD function has a low frequency peak at about 50 kHz and this clusters ceases to appear immediately after the beginning of mechanical loading. Two other clusters have similar features as those reported in [15, 17, 18, 23] for various alloys. The AE cluster 2, which is composed of low frequency transient signals with high amplitude, is associated with twinning. The AE cluster 3 is attributed to dislocation slip. This cluster is formed by lower amplitude members exhibiting the broadband spectrum with the relatively high frequency PSD peak. Some heuristic controversy appears with previously reported results where, in line with common belief and reasonable expectations, the high amplitude high frequency signals were associated with twinning and low amplitude low frequency signals were attributed to dislocation slip. The present result seem to oppose the common belief that the twins generate high frequency transients. However, this controversy is resolved by realization that the ASK clustering algorithm assigns a signal to a certain cluster solely on the basis of its spectral density. At variance to previous reports, in the present work we used a relatively short 1024 points realizations of AE signals for the analysis, i.e. the spectral density was computed per record of 0.5 ms duration. This inevitably results in significant contribution of low-frequency AE signal reverberations into the resultant PSD which is particularly pronounced for high amplitude signals. This shifts the PSD function for twining to lower frequency domain.

As a matter of fact twins nucleate very fast at the substantial fraction of the velocity of sound. Considering their length limited to the grain size, the nucleation time varies form a few nano-seconds to a few microseconds. In this sense the impact of elastic waves generated by mechanical twins on the transducer is comparable to that of delta-source. In other words, twins generate waveforms with a very short rise time but a very broad power spectrum. As a result, the piezoelectric AE receiver is excited at all its resonances with maximum for the PICO sensor used at around 180-200 kHz, which is clearly seen in Figure 3. Therefore, some deviation in the PSD appearance for dislocation slip and twinning is explained by the use of short realizations of the analysis. The issue related to optimal (and well-justified) choice of the length of the realization for spectral analysis and statistical clustering has yet to be addressed and additional experimental and theoretical investigations are still needed. This will be a scope of the future research. Nonetheless, the self-consistent have been obtained in the series of experiments in the present work, which are in general agreement with the previously reported results. In a brief summary, during the first tension-compression cycle we systematically observed the following AE features accompanying active deformation mechanisms in the alloy ZK60:

- The AE signals corresponding to dislocation slip and twining commence almost immediately after the beginning of loading at approximately the same stress because of small difference of their critical resolved shear stress. In the present experiments some signals attributed to twins appeared in the early deformation stage. The overall activity of the dislocation slip on the first tensile half-cycle is appreciable higher than that for twining which is found to be in excellent agreement with direct video observations.
- The energy of AE, both for twinning and dislocation slip, drops during unloading to 0 MPa after the first tension phase of the cycle, Fig. 4b; the cumulative energy for both mechanisms levels out at this stage.
- Profuse twinning and scarce slip features are seen in thy AE time series during compression, which is also in line with direct observations.
- The dislocation slip-like signals, which are systematically observed during unloading stage can be associated with detwining. The latter has long been recognized as a processes which, unlike twinning, is not accompanied by high amplitude transient AE [11],[16]. Rather it is accompanied by low amplitude fluctuating AE caused by dislocation activity that is seen during twin shrinkage.

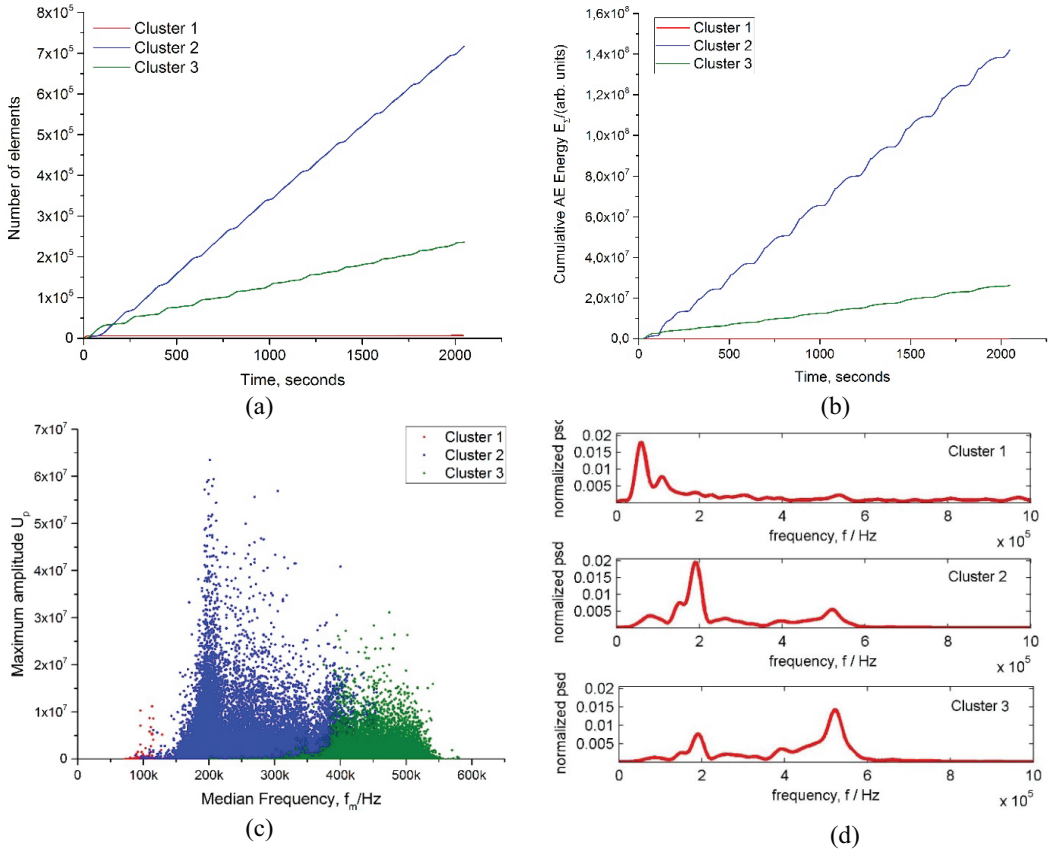

Figure 4: AE clustering result for the whole tension-compression test: (a) cumulative number of members in the cluster; (b) cumulative AE energy for signals belonging to different clusters; (c) maximum amplitude; (d) PSD functions corresponding to the cluster centroids.

Hence, according to both visual observations and AE data, the significant asymmetry in the behavior of active deformation mechanisms can be confirmed during the first loading cycle. While profuse twinning controls the compression loading stage, the dislocation slip mediates the tension deformation stage.

Further cycling results in considerable changes in the AE behavior and corresponding visual observations. For example, at the 10^{th} cycle visual observations show that only intensive detwinning occurs during tension while the compression phase of the cycle is still governed by twinning. Furthermore, more and more twins appears at each following cycle. This can be plausibly explained by the polar nature of twinning and activation of different twinning variants during tension and compression.

The same behaviour is revealed by the AE cluster analysis. At the 10^{th} cycle the AE shows that the twinning dominates both the compression and tension loading stages with only some visible traces of dislocation slip. During unloading to 0 MPa, the number of members (elements) in the corresponding clusters increases for both mechanisms, while the cumulative energy changes appreciably only after compression.

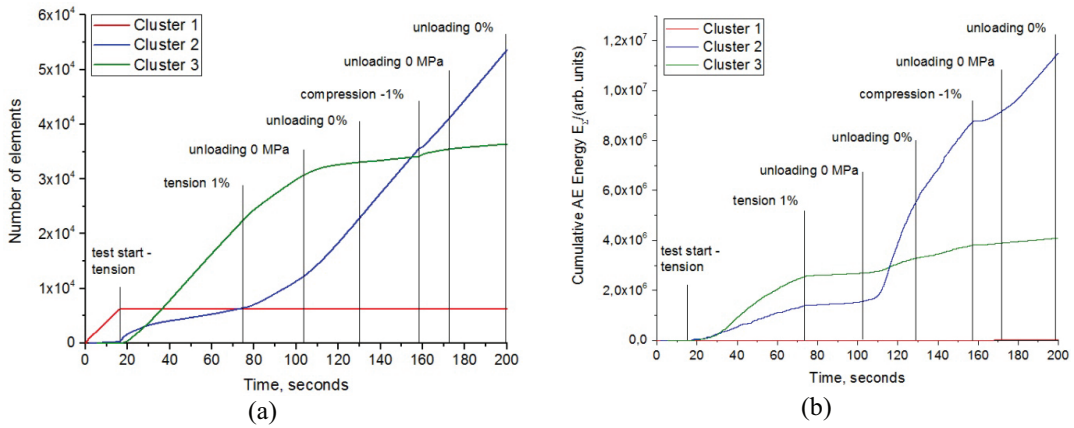

(a) (b)

Figure 5: Results of AE cluster analysis for the first tension-compression cycle: (a) number of elements (members) in cluster; (b) corresponding cumulative AE energy for individual AE clusters representing different operative mechanisms.

3.2. Compression-tension cycle.

During the cyclic deformation with compression-tension loading the visual observations at the first cycle are similar to those during tension-compression, Figure 5 (cf. Figure 2): profuse twinning dominates the compression phase of the cycle while dislocation slip with some twinning in favorable grains governs the strain hardening during tension. No visual changes on the surface can be notice during unloading to 0 MPa.

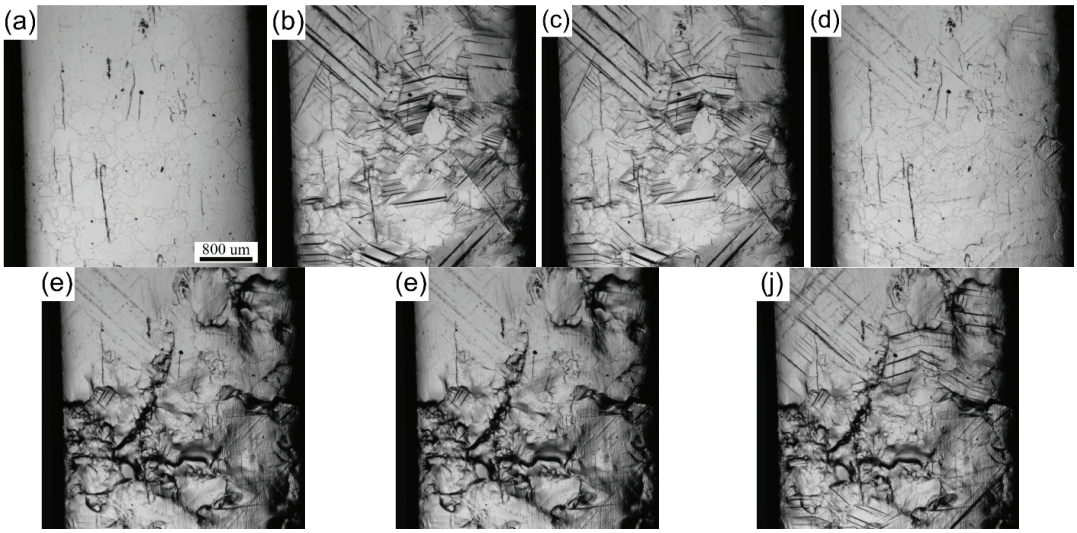

Figure 6: Successive optical video images for the first compression-tension cycle: (a) initial surface; (b) compression to -1% total strain; (c) unloading to 0 MPa; (d) unloading to 0% strain; (e) tension to 1% strain; (f) unloading to 0 MPa; (j) unloading to 0% strain.

The AE signal categorization by the ASK procedure renders qualitatively similar results to those obtained in tension-compression cyclic loading. The following AE clusters with same features in their spectral density and waveforms were consistently recognized, Figure 6: cluster 1 – background noise; 2 – dislocation slip; 3 – twinning.

Figure 7 illustrates the behavior of individual AE clusters during the first deformation cycle.

This can be summarized in brief as follows:

- The activity of mechanical twinning is by far higher than that of dislocation slip during compression.
- The AE energy drops regardless of the deformation mechanisms during unloading to o MPa after compression.
- During the tension phase of the loading cycle, it is the dislocation slip that controls the strain hardening behavior while twining is seen relatively seldom.
- Unloading to o MPa after tension occurs again with significantly lower energy, which is reasonable for the unloading stage; the AE on unloading stage in Mg alloys does not vanish (unlike that in fcc and bcc metals) which is associated with the detwinning of favorably oriented extension twins.

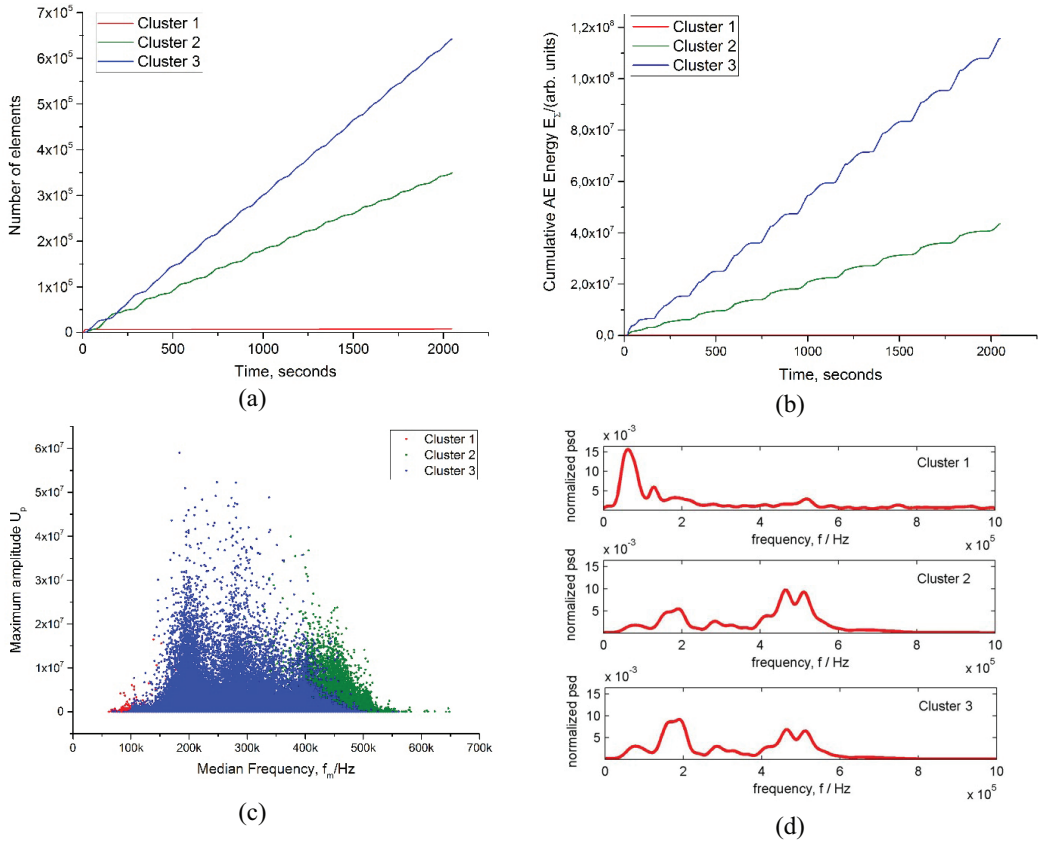

Figure 7: AE clustering result for the whole compression- tension test: (a) cumulative number of members in the cluster; (b) cumulative AE energy for signals belonging to different clusters; (c) maximum amplitude; (d) PSD functions corresponding to the cluster centroids.

At the 10^{th} compression-tension cycle the visual observations resemble those for the tension-compression testing cycle. Profuse twinning at compression stage and

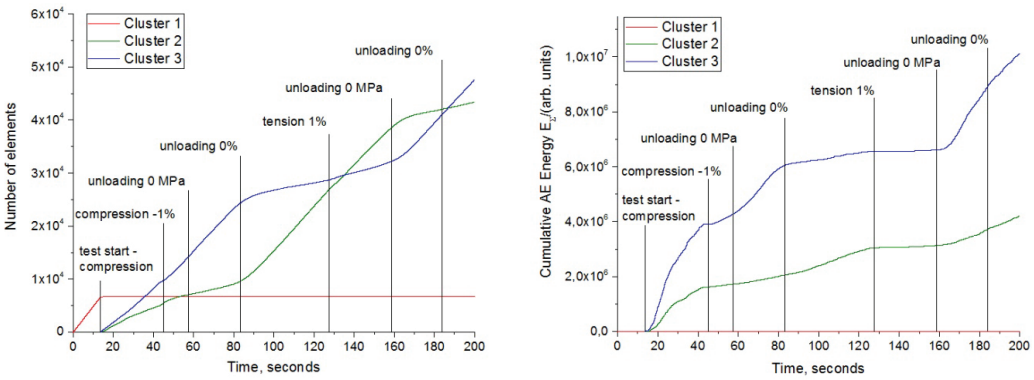

(a) (b)

Figure 8: Results of AE cluster analysis for the first compression- tension cycle: (a) number of elements (members) in cluster; (b) corresponding cumulative AE energy for individual AE clusters representing different operative mechanisms.

detwinning during tension are commonly seen. AE data undoubtedly reflect the dominant activity of twinning and less significant, but never nullified, activity of dislocation slip during compression. The contributions of both mechanisms into the resultant AE signals on the tensile stage is approximately equal and equal activity of these mechanisms during tension. Both mechanisms show a systematic trend towards reduction of their energy with increasing number of cycles which is commonly explained by strain hardening and accumulation of dislocations and twins in the deformed volume that shortens the dislocation mean free pat and reduces the length of newly appearing twins. Furthermore, twining has a natural trend towards saturation since only a limited strain can be accommodated by mechanical twins in the hcp lattice (a maximum extension of 6.4 %, as calculated theoretically by Kocks and Westlake [24]).

3.3. Discussion

A summary of comparison of AE data and visual observations is presented schematically in table 1. One should notice an excellent agreement between the results obtained by different methods. A good convergence of two methods - direct and indirect – provides a high confidence for interpretation of the AE data. The AE technique returns more detailed information about the kinetics of deformation mechanisms if compared to video observations. While only twinning might be seen at a given magnification in some grains, the AE signal can uncover dislocation sources of plastic deformation operating concurrently with mechanical twining in the same or different grains which is hardly seen due to limited optical resolution. Furthermore, AE captures all twinning-related and a large part of slip –related events in the whole deforming volume while the direct video observations are restricted to a small part of the observed surface.

Extending the results of local observations to the entire specimen is, of course, a crude approximation while AE helps to reconstruct the integral picture of deformation kinetics.

The asymmetry of the hysteresis loops shape and their evolution during cyclic deformation, such as that seen in Figure 1, can exert a significant detrimental effect on the overall fatigue performance of Mg alloys, particularly in low-cyclic regime [25]. First of all, one can notice that the considerable tensile mean stress is formed during deformation cycle due to the asymmetry of twining response to the direction of loading. The AE analysis shows undoubtedly that the defects accumulation occurs also differently on different half-cycles. A greater part of twins is formed during compression stage of cyclic loading with constant strain amplitude. A part of them can then elastically relax and detwin during tension, which is reflected in both the hysteresis loop change and in the AE signal. The effect of the early stages of deformation on fatigue resistance in Mg alloys has been just scarcely studied and has yet to be understood.

Table 1: Activity of different deformation mechanisms during the first deformation cycle of the alloy ZK30 (the total strain amplitude is 0.01).

Loading direction	Cycle Number	Activity of deformation mechanism according to AE data		Activity of deformation mechanism according to visual observations
		Twinning	Dislocation slip	
Compression	1	+++	++	T
	10	+++	++	T
Tension	1	+	++	S, T
	10	+++	+	DT
Compression after tension	1	+++	+	T
	10	+++	+	T
Tension after compression	1	+	++	S, T
	10	++	++	DT
Notations: (-) - no activity; (+) - low activity; (++) - intermediate activity; (+++) significant activity; T – twinning, S – slip, DT – detwinning,				

4. Conclusions

In this study, an advanced method of acoustic emission paired with in-situ video observation was used to determine the underlying mechanism during cyclic loading of ZK30 alloy. It has been found that AE data is in good agreement with direct visual observations, ensuring the possibility of using this technique as in-situ method of monitoring magnesium alloys.

Since the beginning of cyclic deformation coarse grain ZK30 alloy exhibits significant asymmetry in tension-compression behavior and underlying mechanisms. While intensive macro plastic strain accompanied with dislocation slip, formation of considerable surface relief and trace twins during tension, compression is governed by profuse twinning. After the first deformation cycle hysteresis loop undergoes significant changes in tension area, associated with evolution of deformation mechanisms and shift of the twinning start point. Such an asymmetry is a result of different twinning planes during tension and compression and can partly describe fatigue phenomenon in magnesium – a major part of defects is formed during compression stage of cyclic loading and then elastically relaxed during the tension. Moreover, these effects lead to the formation of positive median stresses during loading, which obviously decrease the overall fatigue life.

Acknowledgements

Financial support from the Russian Science Foundation through the grant-in-aid No.15-19-30025 is gratefully appreciated.

References

[1] Roberts, C.S. 1960 *Magnesium and its alloys*. Wiley: New York p 230

[2] Stanford, N.; Sotoudeh, K.; Bate, P.S. 2011 Deformation mechanisms and plastic anisotropy in magnesium alloy AZ31. *Acta Materialia* **59** pp 4866-4874.

[3] Chamos, A.N.; Pantelakis, S.G.; Haidemenopoulos, G.N.; Kamoutsi, E. 2008 Tensile and fatigue behaviour of wrought magnesium alloys AZ31 and AZ61. *Fatigue and Fracture of Engineering Materials and Structures* **31** pp 812-821.

[4] Yoo, M. 1981 Slip, twinning, and fracture in hexagonal close-packed metals. *Metall and Mat Trans A* **12** pp 409-418.

[5] Lou, X.Y.; Li, M.; Boger, R.K.; Agnew, S.R.; Wagoner, R.H. 2007 Hardening evolution of AZ31b mg sheet. *International Journal of Plasticity* **23** pp 44-86.

[6] Taylor, G.I. 1938 Plastic strain in metals. *J. Inst. Metals* **LXII** 307-324.

[7] Christian, J.W.; Mahajan, S. 1995 Deformation twinning. *Progress in Mater. Sci.* **39** pp 1-157.

[8] Barnett, M.R. 2007 Twinning and the ductility of magnesium alloys. Part I "Tension" twins. *Materials Science and Engineering A* **464** pp 1-7.

[9] Barnett, M.R. 2007 Twinning and the ductility of magnesium alloys. Part II. "Contraction" twins. *Materials Science and Engineering A* **464** pp 8-16.

[10] Wu, L.; Jain, A.; Brown, D.W.; Stoica, G.M.; Agnew, S.R.; Clausen, B.; Fielden, D.E.; Liaw, P.K. 2008 Twinning–detwinning behavior during the strain-controlled low-cycle fatigue testing of a wrought magnesium alloy, ZK60a. *Acta Materialia* **56** pp 688-695.

[11] Vinogradov, A.; Orlov, D.; Danyuk, A.; Estrin, Y. 2015 Deformation mechanisms underlying tension–compression asymmetry in magnesium alloy ZK60 revealed by acoustic emission monitoring. *Materials Science and Engineering: A* **621** pp 243-251.

[12] Yu, Q.; Zhang, J.; Jiang, Y. 2011 Direct observation of twinning–detwinning–retwinning on magnesium single crystal subjected to strain-controlled cyclic tension–compression in [0001] direction. *Philosophical Magazine Letters* **91** pp 757-765.

[13] Vinogradov, A.; Vasilev, E.; Seleznev, M.; Máthis, K.; Orlov, D.; Merson, D. 2016 On the limits of acoustic emission detectability for twinning. *Materials Letters 183* pp 417-419.

[14] Mathis, K.; Chmelik, F.; Janecek, M.; Hadzima, B.; Trojanova, Z.; Lukac, P. 2006 Investigating deformation processes in AM60 magnesium alloy using the acoustic emission technique. *Acta Materialia* **54** pp 5361-5366.

[15] Máthis, K.; Csiszár, G.; Čapek, J.; Gubicza, J.; Clausen, B.; Lukáš, P.; Vinogradov, A.; Agnew, S.R. 2015 Effect of the loading mode on the evolution of the deformation mechanisms in randomly textured magnesium polycrystals – comparison of experimental and modeling results. *International Journal of Plasticity* **72** pp 127-150.

[16] Drozdenko, D.; Bohlen, J.; Yi, S.; Minárik, P.; Chmelík, F.; Dobroň, P. 2016 Investigating a twinning–detwinning process in wrought Mg alloys by the acoustic emission technique. *Acta Materialia* **110** pp 103-113.

[17] Vinogradov, A.; Orlov, D.; Danyuk, A.; Estrin, Y. 2013 Effect of grain size on the mechanisms of plastic deformation in wrought Mg–Zn–Zr alloy revealed by acoustic emission measurements. Acta Materialia **61** pp 2044-2056.

[18] Vinogradov, A.; Orlov, D.; Danyuk, A.; Estrin, Y. 2015 Deformation mechanisms underlying tension–compression asymmetry in magnesium alloy ZK60 revealed by acoustic emission monitoring. *Materials Science and Engineering A* **621** pp 243-251.

[19] Seleznev, M.; Vinogradov, A. 2014 Note: High-speed optical imaging powered by acoustic emission triggering. *Rev Sci Instrum* **85** pp 76-103.

[20] Vinogradov, A.; Nadtochiy, M.; Hashimoto, S.; Miura, S. 1995 Acoustic-emission spectrum and its orientation dependence in copper single-crystals. *Materials Trans. JIM* **36** pp 496-503.

[21] Pomponi, E.; Vinogradov, A. 2013 A real-time approach to acoustic emission clustering. *Mech. Syst. Signal Proc.* **40** pp 791-804.

[22] Vinogradov, A.; Merson, D.L.; Patlan, V.; Hashimoto, S. 2003 Effect of solid solution hardening and stacking fault energy on plastic flow and acoustic emission in Cu-Ge alloys. *Materials Science and Engineering A* **341** pp 57-73.

[23] Vinogradov, A.; Vasilev, E.; Linderov, M.; Merson, D. 2016 Evolution of mechanical twinning during cyclic deformation of Mg-Zn-Ca alloys. *Metals* **6** p 304.

[24] Kocks, U.F.; Westlake, D.G. 1967 Importance of twinning for ductility of hcp polycrystals. *Transactions of the Metallurgical Society of AIME* **239** p 1107.

[25] Xiong, Y.; Jiang, Y. 2014 Fatigue of ZK60 magnesium alloy under uniaxial loading. *International Journal of Fatigue* **64** pp 74-83.